

QRFH antenna for VGOS receiver (YQR-03-002)

A. García, O. García-Pérez, F. Tercero

CDT Technical Report 2020-26

Observatorio de Yebes
19080, Guadalajara (Spain)
E-mail: ogarcia@oan.es

Abstract- This report summarizes the Quad-Ridged Feed Horn (QRFH) results for Yebes built model YQR-03-002. It includes preliminary specifications, and interface drawings and experimental results of the manufactured antenna. Reflection, isolation, and radiation patterns have been measured in the 2.2 to 14 GHz frequency range. In addition, aperture efficiency on a VGOS 13.2m ring-focus radio telescope has been estimated by numerical calculations using the measured radiation patterns as input.



November, 2020

Contents

Contents	3
1 Introduction	4
2 Mechanical interface	6
3 Feed assembly.....	7
4 Feed measurements.....	8
4.1 Port reflection and isolation	8
4.2 Radiation patterns	9
4.3 Phase center	10
5 Aperture efficiency	11
References	13
Appendix A. Radiation patterns	15

1 Introduction

This document presents the development of an antenna feed to be part of a VGOS broadband receiver. The feed follows a broadband dual-polarized QRFH topology, which is being widely utilized in many broadband radio astronomy systems [1][2].

The electrical design has been carried out by optimizing the horn and ridge's profiles. The goals for the optimization were input reflection losses under a given threshold, and aperture efficiency on the reflector as high as possible. Two SMA compatible connectors are used to get both linear orthogonal polarizations.

The antenna has been manufactured by the Spanish industry, whereas the design and tests have been carried out at Yebes Observatory. The antenna description and specifications, as well as the measured parameters are summarized in Table I.

Project	VGOS [3]
Application	Antenna Feed for VGOS 13.2m radio telescope
S/N	YQR-03-002
Manufactured date	2020 October
Measured date	2020 November
Output	2 coaxial SMA type
Reference impedance	50 Ω
Frequency	2.2-14 GHz
	Measured
Port reflection(typ.)	-11 dB
(max.)	-10 dB
Port isolation (min.)	29 dB
Mean aperture efficiency over VGOS radio telescope (calculated from measurements)	60 %
Xpolar (min.)	30 dB

Table I. Summary of specifications and results of the manufactured QRFH antenna.



Fig. 1.1. Picture of the QRFH antenna.

2 Mechanical interface

The antenna consists of an external horn and four internal ridges (QRFH [2]), whose profiles are defined by analytical curves. The ridges slightly protrude above the horn at the end of the aperture. However, for convenience, the aperture has been defined as the edge of the horn profile. The antenna also has a transition between the quad-ridged waveguide and the two coaxial ports. At the bottom of the antenna there is a cover with the appropriate interface to attach the antenna at the cold stage of the cryostat. The antenna is entirely made of aluminum.

Fig. 2.1 shows the overall dimensions of the antenna, including the distances from the bottom to the limit of the ridges, the aperture, the phase center (the calculation of its position is described in Section 4.3) and the two coaxial ports respectively. The interface view at the bottom of the antenna is shown in Fig. 2.2. Ports position from an isometric view is shown in Fig. 2.3.

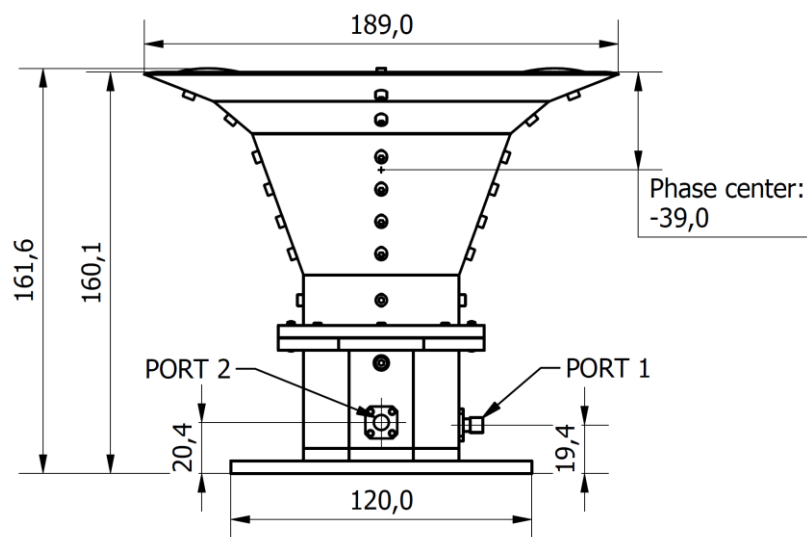


Fig. 2.1. Overall dimensions of the QRFH antenna.

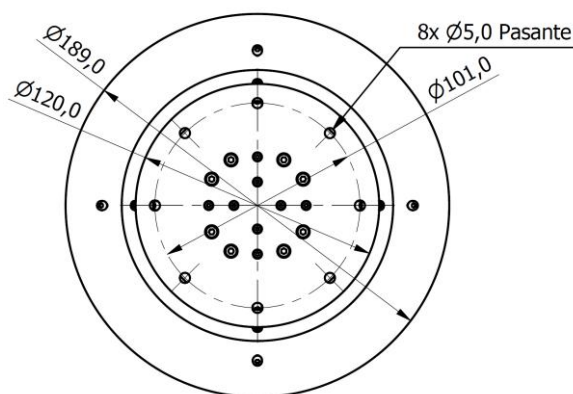


Fig. 2.2. Bottom interface of the QRFH antenna.

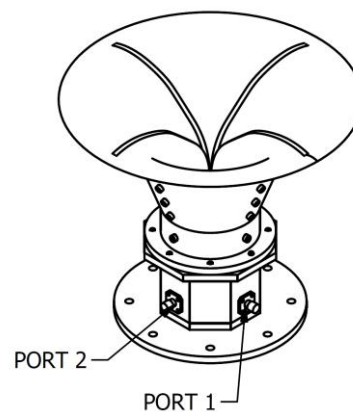


Fig. 2.3. Isometric view of the QRFH antenna.

3 Feed assembly

No issues were noticed during assembly, though port 1 showed suboptimal behavior during the measurement (see figure 3.1). After disassembling said port, straightening the wire and cleaning the hole again using compressed air, the expected reflection coefficient was obtained (see figure 4.1) showing better than -10dB reflection in the whole band.

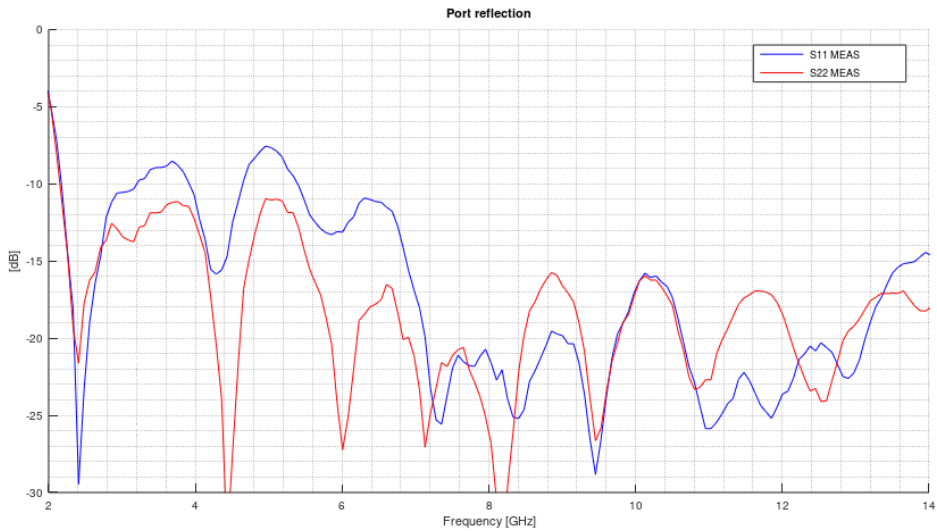


Fig. 3.1. Measured reflection after first assembly

The gap between the ridges was measured as 400um to 450um for the “a” cut and 400um for the “b” cut.

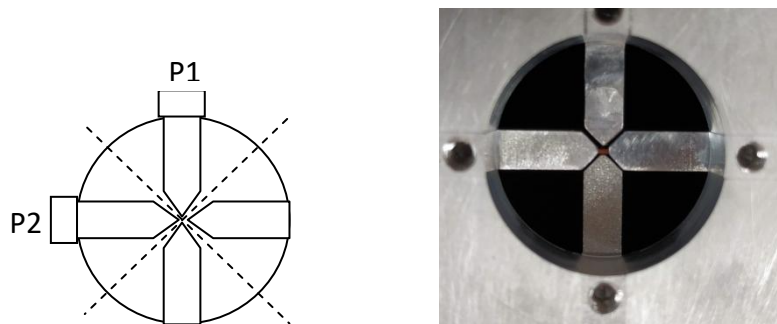


Fig. 3.2. Bottom view. Picture and diagram

4 Feed measurements

4.1 Port reflection and isolation

The return losses have been measured at the output coaxial connectors, obtaining the results shown in Fig. 4.1. On the other hand, the isolation between both ports is shown in Fig. 4.2.

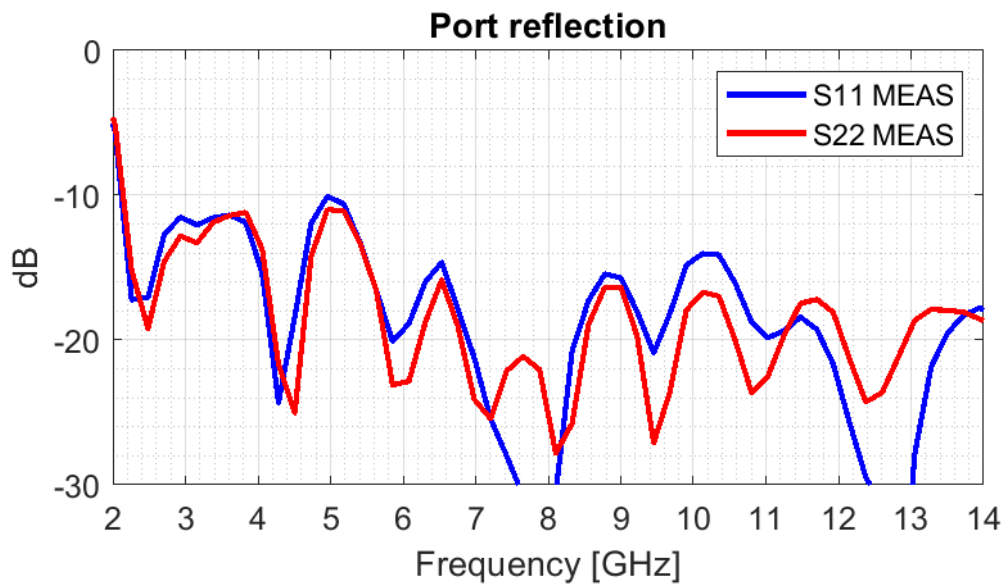


Fig. 4.1. Measured port reflection.

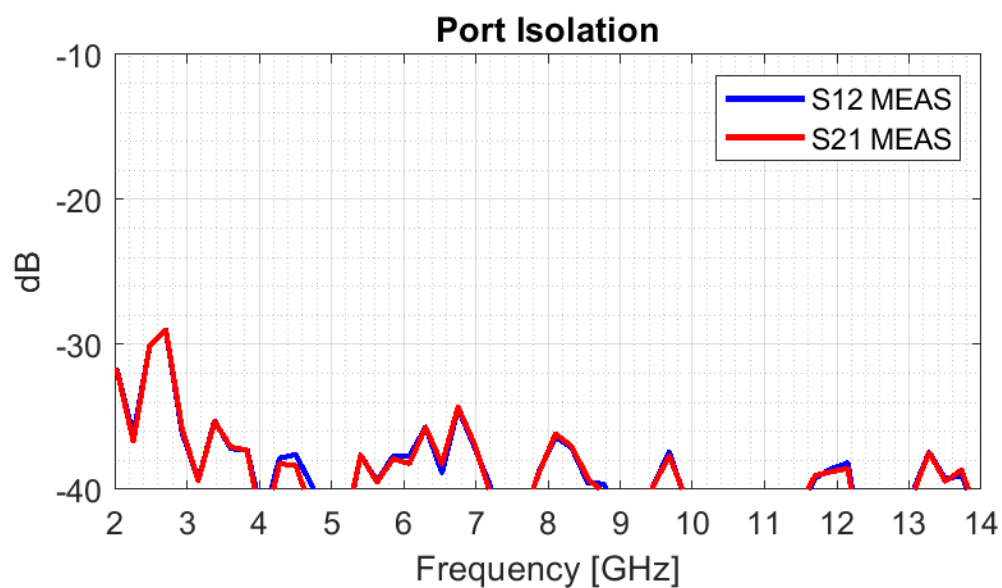


Fig. 4.2. Measured port isolation.

4.2 Radiation patterns

The measurement of the antenna radiation patterns has been performed at the anechoic chamber of Yebes (CDTAC) (Fig. 4.3)[4].

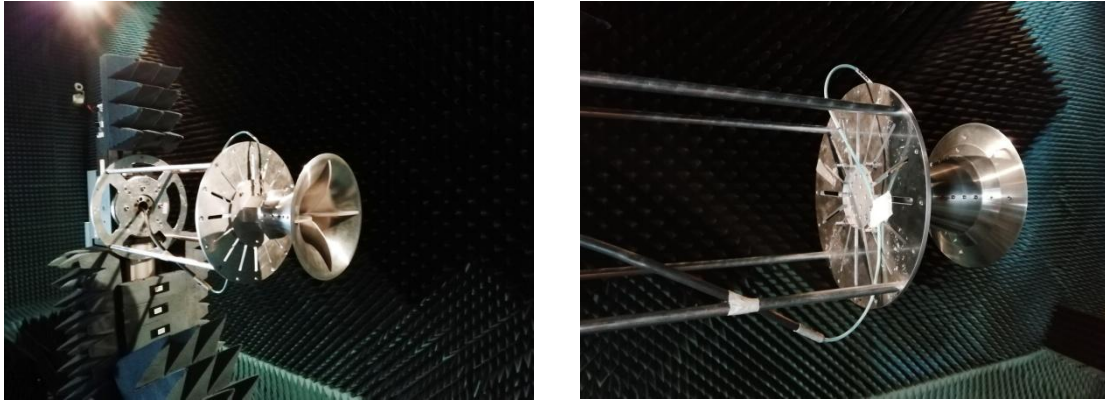


Fig. 4.3. Measurement of the QRFH in the anechoic chamber of Yebes (CDTAC).

It is a broadband antenna, so it has been necessary to use several probes for the measurements, since each probe works in a specific frequency band. The different probes that were used, and the frequency bands measured with each one, are shown in Table II.

Probe	Frequency band	Delta	Frequency points
WR430	2-3 GHz	0.5 GHz*	4
WR229	3.5-4.5 GHz	0.5 GHz	3
WR159	5-7 GHz	0.5 GHz	5
WR112	7.5-10 GHz	0.5 GHz	6
WR75	10.5-15 GHz	0.5 GHz	10

(*) 2.0, 2.2, 2.5, 3.0 GHz

Table II. Antenna probes used for the radiation pattern measurements.

The measurement has been done with the Spherical Near Field System, with two linear polarizations (LIN-0(Ex) and LIN-90(Ey)). Each antenna port has been measured separately, loading the other port with 50 Ω .

The complete set of measured radiation patterns of the antenna are plotted in the Appendix A. The cuts at 0, 45 and 90 degrees are shown, corresponding to the E, D and H planes respectively. The E-Plane is the one aligned with the port.

4.3 Phase center

The location of the phase centre, as a function of frequency, obtained from the measured radiation patterns is plotted in Fig. 4.4. This position has been defined with respect to the aperture, in such a way that negative values correspond to positions inside the horn.

The optimal position of the feed with respect the focus of the radio telescope has been calculated as the one that maximized the average aperture efficiency in the broad band. The obtained values were -38.8 mm and -39.2 mm for port 1 and 2 respectively, which means that the optimal for this antenna is about -39.0 mm from the aperture (the tolerances in the measurement are in the order of 1 mm).

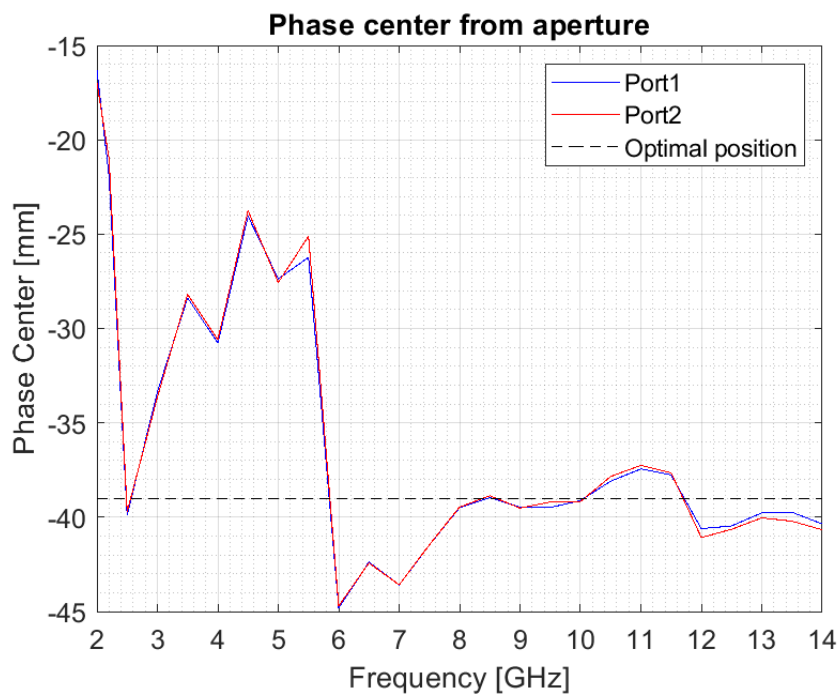


Fig. 4.4. Measured phase center position with respect to the aperture.

5 Aperture efficiency

The aperture efficiency of the VGOS 13.2m reflector antenna illuminated by the QRFH antenna can be calculated using the measured radiation patterns of the feed. The parameters of the VGOS antenna used for the calculation are the following:

- Antenna type: Ring Focus [5][6]
- Subtended half-angle: 65°
- Diameter of the parabola: 13.2 m
- Focal length: 3.7 m
- Subreflector diameter: 1.48 m

The aperture efficiency has been calculated analytically, with the expressions in [7]-[8]. The results obtained from the analytical expressions have also been reproduced with optical physics, using GRASP, without significant differences. The overall aperture efficiency of each antenna port is shown in Fig. 5.1. In Fig. 5.2 the aperture efficiency is decomposed by a set of subefficiencies: illumination, spill-over, polarization and phase.

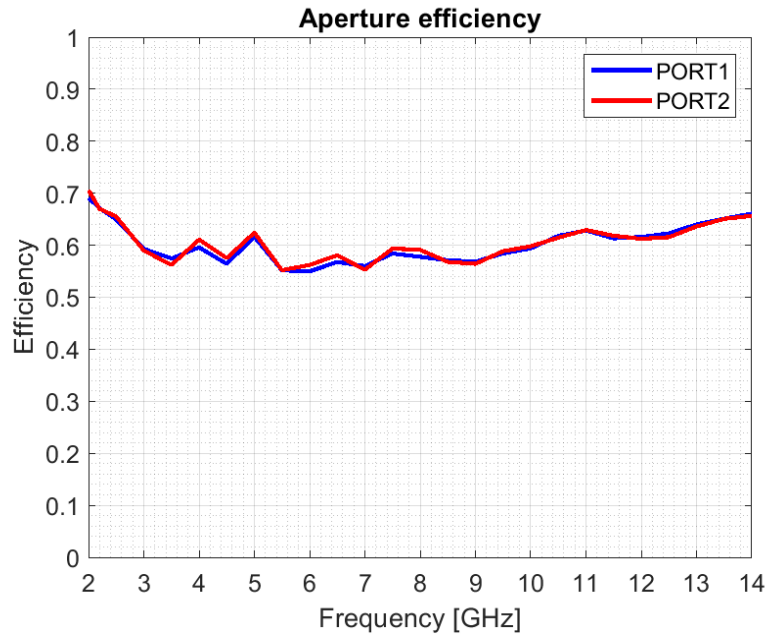


Fig. 5.1. Estimated aperture efficiency of the QRFH antenna for each port.

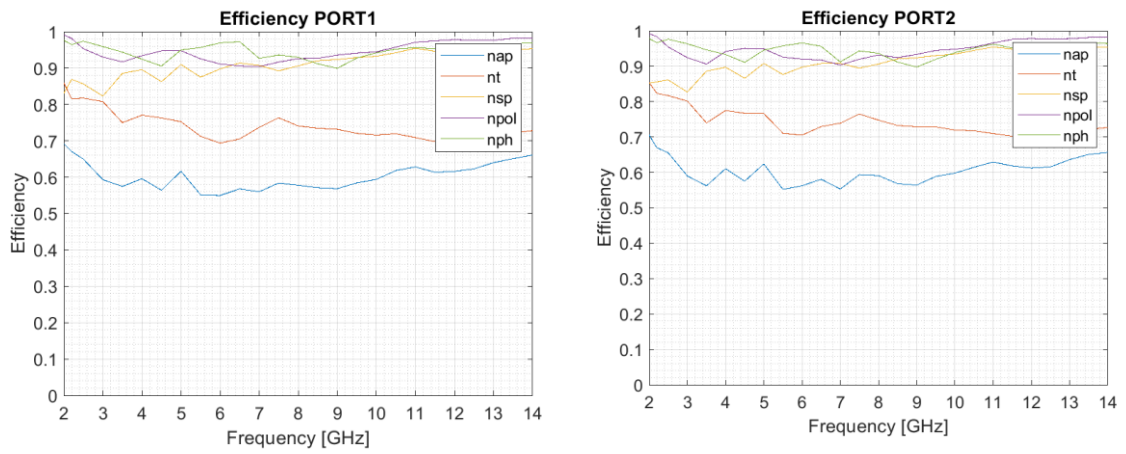


Fig. 5.2. Estimated subefficiencies of QRFH antenna for each port.

References

- [1] A. H. Akgiray, in *New Technologies Driving Decade-Bandwidth Radio Astronomy: Quad-Ridged Flared Horn & Compound-Semiconductor LNAs*, Pasadena, California, 2013, pp. 67-72.
- [2] A. Akgiray, S. Weinreb, W. A. Imbriale and C. Beaudoin, "Circular Quadruple-Ridged Flared Horn Achieving Near-Constant Beamwidth Over Multioctave Bandwidth: Design and Measurements," *IEEE Transactions on Antennas and Propagation*, vol. 61, no. 3, pp. 1099-1108, March 2013.
- [3] B. Petrachenko, "VLBI2010: Progress and Challenges," *IVS 2012 General Meeting Proceedings*, pp. 42-46, 2012.
- [4] J. M. Serna, F. Tercero, T. Finn and J. A. López, "The CDT Ultra Wide-Band Anechoic Chamber," *European Conference on Antennas and Propagation*, 2011.
- [5] T. Milligan, "A Simple Procedure for the Design of Classical Displaced-Axis Dual-Reflector Antennas Using a Set of Geometric Parameters," *IEEE Antennas and Propagation Magazine*, vol. 41, no. 6, pp. 64-71, December 1999.
- [6] T. Milligan and A. P. Popov, "Amplitude Aperture-Distribution Control in Displaced-Axis Two-Reflector Antennas," *IEEE Antennas and Propagation Magazine*, vol. 39, no. 6, pp. 58-63, December 1997.
- [7] A. P. Popov and T. Milligan, "Amplitude Aperture-Distribution Control on Displaced-Axis Two-Reflector Antennas," *IEEE Antennas and Propagation Magazine*, vol. 39, no. 6, pp. 58-63, December 1997.
- [8] in *Modal-Based Design Techniques for Circular Quadruple-Ridged Flared Horn Antennas*, 2015, pp. 7-10.
- [9] M. A. Campo, F. J. del Rey, J. L. Besada and L. de Haro, "SABOR: Description of the Methods Applied for a Fast Analysis of Horn and Reflector Antennas," *IEEE Antennas and Propagation Magazine*, vol. 40, no. 4, pp. 95-108, August 1998.
- [10] P.-S. Kildal, "Factorization of the Feed Efficiency of Paraboloids and Cassegrain Antennas," *IEEE Transactions on antennas and propagation*, Vols. AP-33, no. 8, pp. 903-908, August 1985.

- [11] F. Tercero et al., "Optimization of the Quad-Ridged Horn for the geodetic VGOS station of the Yebes Observatory," *European Conference on Antennas and Propagation*, 2018.

Appendix A. Radiation patterns

